Chapter 4

High-Density, Multiplexed Patterning of Cells at Single-Cell Resolution for Applications in Tissue Engineering

"To further the construction of complex tissues, or even entire organs, there are still significant technical challenges to overcome. Among them, a very important problem is subtly combining and orchestrating cells, growth factors and scaffolds into an architecture that will allow their unfettered interaction, especially where distinct cell types are required in anatomically exact locations to attain biological function."

-Thomas Boland. Inkjet printing of viable mammalian cells. *Biomaterials,* **2005,** 26, 93-99.

4.1 Introduction

4.1.1 Advances in tissue engineering

Considerable advances in the design of functional replacements for damaged or destroyed tissues and organs over the last decade or so have created an avenue for overcoming both the shortage and immunogenicity of allogeneic transplants. Tissue

engineered substitutes for a number of tissues have already been created, including stomach[1], esophagus[2], spinal cord[3], and several types of commercially available skin. In addition, various types of cartilage, bone, and blood vessel replacements have been successfully implanted into humans[4].

Classical tissue engineering approaches have utilized a top-down approach, in which a solid scaffold mimicking an organ or tissue is first created, followed by seeding of cells on this scaffold[5]. While this method has been useful in a broad range of scenarios, its major limitations are difficulties in mimicking the native microarchitecture (i.e., placing different cell types in precise positions relative to each other) and vascularizing large scaffolds for delivery of oxygen and nutrients to cells[6].

An alternative to this approach, which has been developed in recent years, is a bottom-up approach, in which cells are first patterned in an arrangement that closely emulates the native tissue microarchitecture, and these building blocks are then "stacked" together to create a functional tissue unit[7]. Examples of this include encasing patterned cells in thin layers of thermally- or UV-curable hydrogels, which are sufficiently rigid so as to maintain, intact, the architecture of patterned cells. These cell-laden hydrogels are then stacked on top of each other to create three-dimensional structures[8].

The success of cell culture and growth in these environments lies in the fact that hydrogels can closely mimic the tensile, elastic, and compressive physical forces a cell typically encounters within its native extracellular matrix (ECM) [9]. In addition, hydrogels can be impregnated with ECM proteins that allow cells to attach to the extracellular matrix (be it native or synthetic), and which provide the chemical cues that anchorage-dependent cells require for growth and survival[9-11]. Moreover, soft-lithography

techniques can be used to imprint vascular channels between cell-laden hydrogel layers to provide perfusion at the length-scales of the native microenvironment[12].

An important additional benefit that certain hydrogels can provide is their relative lack of immunogenicity, which could potentially allow allogeneic cells encased within them to be transplanted with minimal risk of detection by the host's immune surveillance[13,14]. Capitalizing on this idea, many groups have sought to minimize or even eliminate the immunogenicity of allogeneic islet transplants by encapsulating donor β cells (insulin-producing islet cells) in hydrogel microcapsules made of non-immunogenic materials, such as alginate or polyethylene glycol (PEG) [15-17]. These hydrogel capsules contain pores that are large enough to allow oxygen and nutrients to be transported freely for metabolic sustenance, but that are too small for entry of antibodies or T cells[14]. In principle, islets from other species (pigs, monkeys) could potentially be encapsulated, without the danger of graft rejection, allowing for an ample supply of islets to be harvested and transplanted[10]. In addition, human and non-human stem- and precursor-cells could be propagated in culture and then encapsulated for transplantation[10,14].

Of course, the potential advantages of encapsulation come with the challenges of ensuring cell survival in microcapsules over extended periods. Many groups have looked at ways of increasing the longevity of cells within these capsules by adding extracellular matrix proteins, tuning their size (smaller capsules have a smaller diffusion barrier) and porosity, and embedding molecules (such as VEGF) that accelerate vascularization of the transplants in rodent models.

However, it is becoming increasingly recognized that these may not be the only factors that are essential to cell survival and function. In most tissues, cells require

chemical cues from particular types of adjacent cells (juxtacrine signaling) and nearby cells (paracrine signaling) in order to survive and properly perform their functional roles. For example, in the central nervous system (CNS), glial cells receive inputs, assimilate information and send instructive chemical signals both to neurons and to other neighboring cells[18,19]. Astrocytes, in particular, have been implicated in dynamic regulation of neuron production, synaptic network formation, and neuron electrical activity[20]. Also, in endocrine glands, proper hormone secretion requires cell-cell communication for regulated and synchronous activity of all cells within the gland[21,22]. The human islet is no exception. Unlike the rodent islet, in which β cells cluster together in the islet center (forming an "insulin core") while glucagon-secreting α cells and the less abundant δ and PP cells are relegated to the periphery, all endocrine cell types in human islets are interspersed together in a manner that is likely nonrandom (Figure 4.1). The multiple islet cell types are free to intermingle in "an arrangement which predisposes human islets for strong paracrine interactions[23]." In order for native microarchitectural arrangements to be reproduced in synthetic constructs created from cultured islet or CNS cells, some method of patterning these various cell types in close proximity to each other, in the correct ratios, and with precise relative positioning is needed.

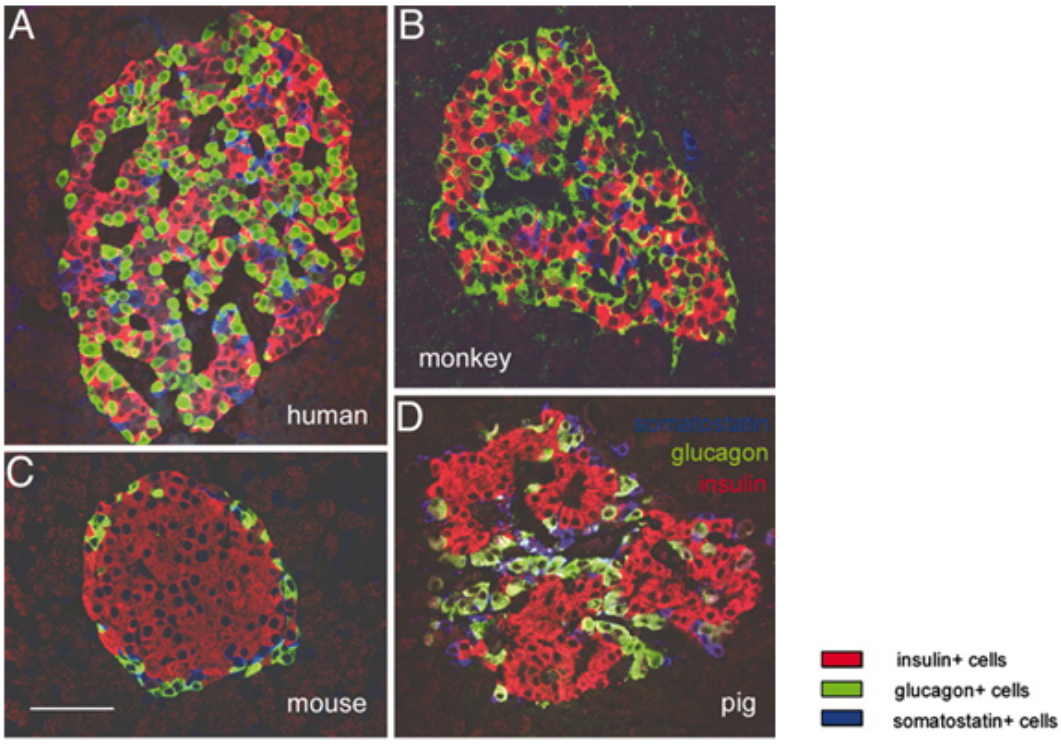

Figure 4.1. Cell arrangements within islets of Langerhans in different species. Note the core-mantle arrangement of α and β cells in mouse and pig islets in contrast to the more dispersed, almost checkerboard-like, clustering of cells in human islets. Red → β cells; Green → α cells; Blue → δ cells.

4.1.2 Challenges and limitations to high-resolution multiplexing

Toward this end, microfabrication techniques borrowed from the semiconductor industry appear to hold the most promise. Microfabrication techniques have paved the way to breakthroughs in our ability to pattern cells at high resolution for applications in biosensing[24,25], drug screening[26,27], neural networks[28], and artificial tissues[29,30]. Existing methods for patterning cells include microcontact printing[31,32], inkjet printing[6,33,34], switchable substrates[35,36], elastomeric stencils[37,38], microwells[29,39], optical tweezers[40,41], electrophoresis[42], and dielectrophoresis[8,43]. A major limitation of most of these platforms,

however, is the multiplexing resolution – the resolution at which different cell types can be patterned. For example, microcontact printing can be used for dense patterning of cell-binding proteins with low-micron to sub-micron feature sizes; however, in order to print distinct features adjacently, multiple inking and alignment steps must be performed. In addition, the loading density of biomolecules patterned by this approach is limited, as the platform is typically suited to printing monolayers. Dielectrophoresis has been successfully used to pattern complex two-dimensional cellular microstructures, including liver lobules[8,43], but this approach does not appear as yet to be amenable to a high degree of multiplexing. Inkjet printing is an exciting approach to high-throughput biomolecule printing, but its application to cell printing is still being tested as there are unanswered questions regarding cell viability in the presence of the thermal and mechanical stresses associated with the printing process. In addition, the feature resolution of biomolecule- and cell-based inkjet printers (~60 – 100 μm) is not yet at the single-cell level[6,33,34].

While microfluidic patterning of substrates for highly multiplexed biological sensing has been demonstrated[44], this technique has not yet been used for high-resolution multiplexing of cells. This is likely due to a number of limitations of current patterning schemes. In the most general case, multiplexed features are created by simply flowing a distinct oligo, protein, antibody, or other biomolecule or chemical into each channel within a microfluidic device. Since microfluidic channels are typically long and thin, they are well-suited to patterning high-aspect ratio features (long, thin lines or rectangles), but not low-aspect ratio features, such as the micron-scale squares or spots that would be needed for high density cell arrays. While it is possible in theory to pattern such features using modifications of the PDMS device architecture, these modifications do not come

without their own set of challenges. For example, one could envisage building a multilayer PDMS structure, such that each layer contains a fluidic network that feeds a unique biomolecule solution to a series of micron-sized spots in the patterning (first) layer[45,46]. However, the task of aligning multiple layers and creating vias connecting the layers reliably is extremely arduous, and therefore impractical for high-density multiplexing of more than 2 – 3 distinct molecules or cells.

4.2 From High Density Microarrays to Single-Cell Resolution Cell Arrays

4.2.1 Creating a dense multiplexed cell microarray

Here we show a relatively straightforward method for circumventing these limitations in microfluidic patterning, thereby facilitating high resolution biomolecule- and cell-multiplexing, while minimizing the complexities of device fabrication and processing time. The approach involves creating a densely-patterned DNA-microarray that is then converted into a dense cell-microarray.

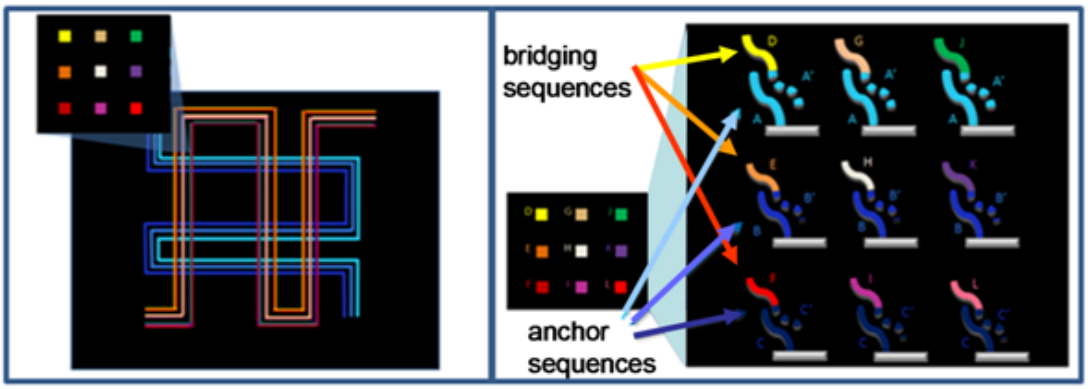

Figure 4.2. The preparation of a high density DNA microarray for tissue assembly. Illustration of the orientation of microfluidic flow patterning molds #1 (blue lines) for deposition of *n* anchor ssDNA sequences, and #2 (red lines) for patterning *m* bridging sequences. The resulting pattern is a series of *n x m* microarrays, with each array spot having its own unique chemical identity.

As shown in **Figure 4.2**, the small DNA microarray features are created in two sequential oligonucleotide flow-patterning steps, as follows: 1. A PDMS device containing a high density of parallel channels is used to flow-pattern distinct oligo strands ("anchor strands") onto a polylysine-coated glass surface. 2. The PDMS stamp is then re-oriented on the substrate 90^{o} clockwise, and a distinct set of oligos are flowed into the PDMS device to create a series of *n x m* microarrays. These oligos are designed to include a 20-base pair "tail" that is complementary to one of the anchor sequences, and a 20-base pair "head" with a unique sequence. As such, after the DNA patterning is complete, these oligos serve as intermediaries that bridge the anchor sequences with unique DNA-conjugated cells. For example, in the first patterning step, we flowed three 80-mer anchor sequences – named **A**, **B**, and **C** – in 3 adjacent channels and simultaneously repeated this flow-patterning arrangement 6 times. In the second patterning step, we flowed three sets of 3 distinct bridging strands, also in 3 adjacent channels (one set per channel): first channel - strand **A'-i** (containing both a 20-mer "tail" sequence that is complementary to anchor strand **A**, and a unique 20-mer "head"

sequence **i**), **B'-ii**, and **C'-iii**; second channel - strands **A'-iv**, **B'-v**, and **C'-vi**; third channel – strands **A'-vii**, **B'-viii**, **C'-ix**. This flow-patterning arrangement was also repeated 6 times simultaneously. The result was a series of thirty-six 3 x 3 arrays, in which each 3 x 3 array contained 9 distinct oligonucleotide "head" sequences (**i, ii, iii, iv, v, vi, vii, viii, ix**) that were available for binding of 9 distinct cell types conjugated to one of 9 complementary strands (**i', ii', iii', iv', v', vi', vii', viii', ix'**). The red squares in **Figure 4.3a** were created by hybridization of **i'**-Cy5 fluorescent DNA to the 3 x 3 array, while green squares were generated by hybridizing (**ii'-ix')**-Cy3 to the array. By adding only **A'-i**, **B'-ii**, and **C'-iii** strands in the second patterning step, creating 3 x 1 arrays was straightforward (**Figure 4.3b**). Red squares, green squares, and yellow squares were created by adding **i'**-Cy5, **iii'**-Cy3, and equal concentrations of **ii'**-Cy5 and **ii'**-Cy3, respectively. The dimensions of the square DNA features comprising the arrays exactly equal the width of the channels used to pattern them. Therefore, since the PDMS flow-patterning channels were 10 μm wide and spaced 30 μm apart, closely-packed 10 μm x 10 μm DNA squares were created that could each accommodate a distinct ~10 μm-diameter single cell.

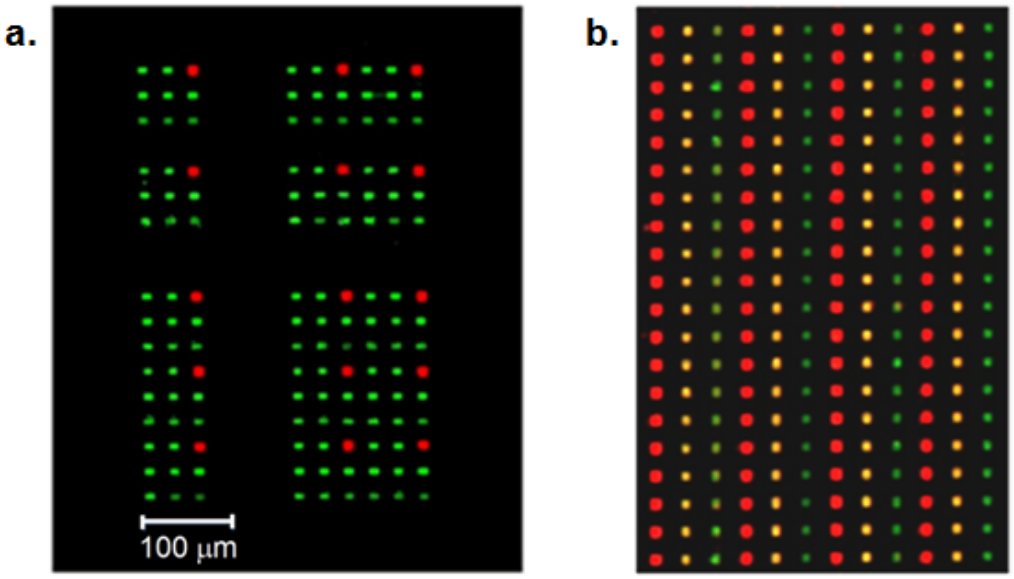

Figure 4.3. Fluorescent scans of high density DNA microarrays. a. Repeating 3 x 3 arrays (red squares = **i** oligomer; green squares = **ii, iii, iv, v, vi, vii, viii,** and **ix** oligomers). **b.** Repeating 3 x 1 arrays (red squares = **i** oligomer; yellow squares = **ii** oligomer; green squares = **iii** oligomer).

To increase the total number of repeats of these 3 x 3 array units, the number of channels in the PDMS flow-patterning device can be increased, or the entire set of channels can be designed to wind up and down in serpentine fashion across the length of the device. For example, by creating serpentine channels with 10 turns, as opposed to straight channels, the number of array repeats can be increased 100-fold (10^2), to thirty-six hundred 3 x 3 arrays.

Once the glass surface was patterned, distinct cell types, each conjugated to one of 9 "head"-complementary oligo sequences, were pipetted onto the surface, where each conjugated cell type bound to its cognate square. Once patterned, the cells were encased in a UV-curable PEG hydrogel so that their positions relative to each other were fixed. The cell-laden hydrogel was then cut into small sections and stacked on top of each other with further curing to create a three-dimensional tissue.

4.2.2 Platform design flexibility and patterning opportunities

In some sense, each DNA square and its cognate cell can be thought of as the biological equivalent of a pixel on a CCD display. The number of possible cell patterns increases exponentially with the number of orthogonal microarray squares in each grid unit - just as the number of patterns that can be displayed on a digital screen scales with the number of pixels. The sizes and spacings of these biological pixels can be tuned by the microfabrication process. More specifically, the feature sizes and spacings can be modified by adjusting the microfluidic channel widths and inter-channel distances, respectively. To allow for physical contact between cells, the feature sizes and inter-feature distances need only be downsized sufficiently. For example, by creating 5 μm-sized square features with 5 μm spacings, a 10 μm-diameter cell attached to its cognate feature will overlap the space between features to a degree, allowing it to come in contact with a neighboring cell whose footprint is also larger than its cognate square. Furthermore, by varying the widths and spacings of channels within a microfluidic device, different-sized features can coexist within the same array, accommodating cells of different sizes. By increasing feature sizes sufficiently, distinct clusters, each containing a few homotypic cells, can be patterned adjacently.

The feature geometries are also tunable to a large extent. For example, one can simply rotate the PDMS device in the second patterning step at an angle between 0^o and 90^o to create parallelograms instead of squares. Rectangles can be created simply by using a microfluidic device in the second patterning step that has different channel widths compared with the device used in the first step. Alternatively, in one of the two patterning steps, a PDMS device can be used in which each channel consists of a series of connected

circles or triangles, allowing a variety of feature shapes to be realized even within the same array unit. Since feature geometry has been shown to influence stem cell fates[32], creating customized feature geometries for each cell type to be arrayed would be very valuable in cases where stem-cells or progenitor-cells are used to pattern tissues. With the flexibility in feature sizes, spacings, and geometries potentially afforded by this platform, dense 2-D microarchitectures can be patterned with feature proximities that permit contact between single cells of varying types, closely mimicking the native tissue environment.

4.2.3 DNA conjugation of cells

In order for a cell type to be addressed to the correct square in a densely-patterned microarray, each cell type had to be labeled with a unique complementary oligonucleotide strand. Previous studies have shown variations of this method. One study showed that oligos could be modified with lipophilic end groups that could anchor the oligos directly into the cell membrane. Bertozzi et al. demonstrated the attachment of ssDNAs to cell-surface glycans by means of Staudinger ligation chemistry, but the initial step required a 3-day cell incubation period with an exogenous modified sugar metabolite to facilitate subsequent chemical steps[47]. More recent work by the same group showed that *N*-hydroxysuccinimidal (NHS) ester-modified DNAs could be reacted directly with amino groups on cell-surface proteins in under an hour[48].

Our approach to conjugating cells with DNA was relatively straightforward (**Figure 4.4**). Cells were biotinylated and then addressed via streptavidin-conjugated oligonucleotides. Our own lab's extensive experience using cysteine-engineered streptavidin (SAC)-conjugated oligos, in conjunction with biotinylated MHC proteins, to

pull down antigen-presenting T cells, inspired this method[49]. Native streptavidin contains a lysine residue in close proximity to the biotin-binding pocket, such that amide coupling strategies for cross-linking DNA would alter the streptavidin-biotin binding capacity. SAC by contrast has been genetically engineered to incorporate a cysteine residue at the carboxy-terminus, away from the biotin-binding pocket, allowing DNA to be conjugated using maleimide chemistry only at this site (since cysteine residues are absent in native streptavidin)[49]. To tailor this strategy for DNA conjugation of cells, cells were first biotinylated (by reacting with NHS-biotin), followed by incubation with their respective SAC-oligos. The advantage of this method is its modularity and ease. The reaction between the SAC-oligos and the biotinylated cells occur immediately upon mixing, so any biotinylated cell can be instantly conjugated with an oligo of one's choosing. For experiments in which cells were patterned on arrays containing different sets of DNAs, biotinylated cells were quickly reacted with the SAC-oligos relevant to each DNA array. In addition, once biotinylated, cells could in theory be passaged a few times and still retain enough surface biotins for sufficient DNA conjugation. This would permit fast DNA-conjugation of cells directly from the culture dish, obviating the need to repeat the biotinylation procedure before every experiment.

Like the conjugation method exemplified by the Bertozzi group[48], our cell conjugation method also constitutes a cell surface marker-free approach. Whereas past cell-patterning approaches utilized antibodies against cell-surface proteins to capture cells (e.g. immunopanning)[50-52], these approaches are only practical if a cell-surface protein exists in sufficient abundance to allow the cell to be held down by surface-bound antibodies[48]. For a marker with less surface density, higher affinity antibodies would be

needed to capture cells. On top of this, producing high-affinity monoclonal antibodies is a time-consuming and expensive process with variable outcomes. By contrast, biotinylation of cells, followed by binding of SAC-oligos, is a simple, generalizable platform that can be used on any cell type, regardless of whether the cell has a targetable surface marker. The cell need only have surface amino groups, which are ubiquitous due to the abundance of membrane proteins.

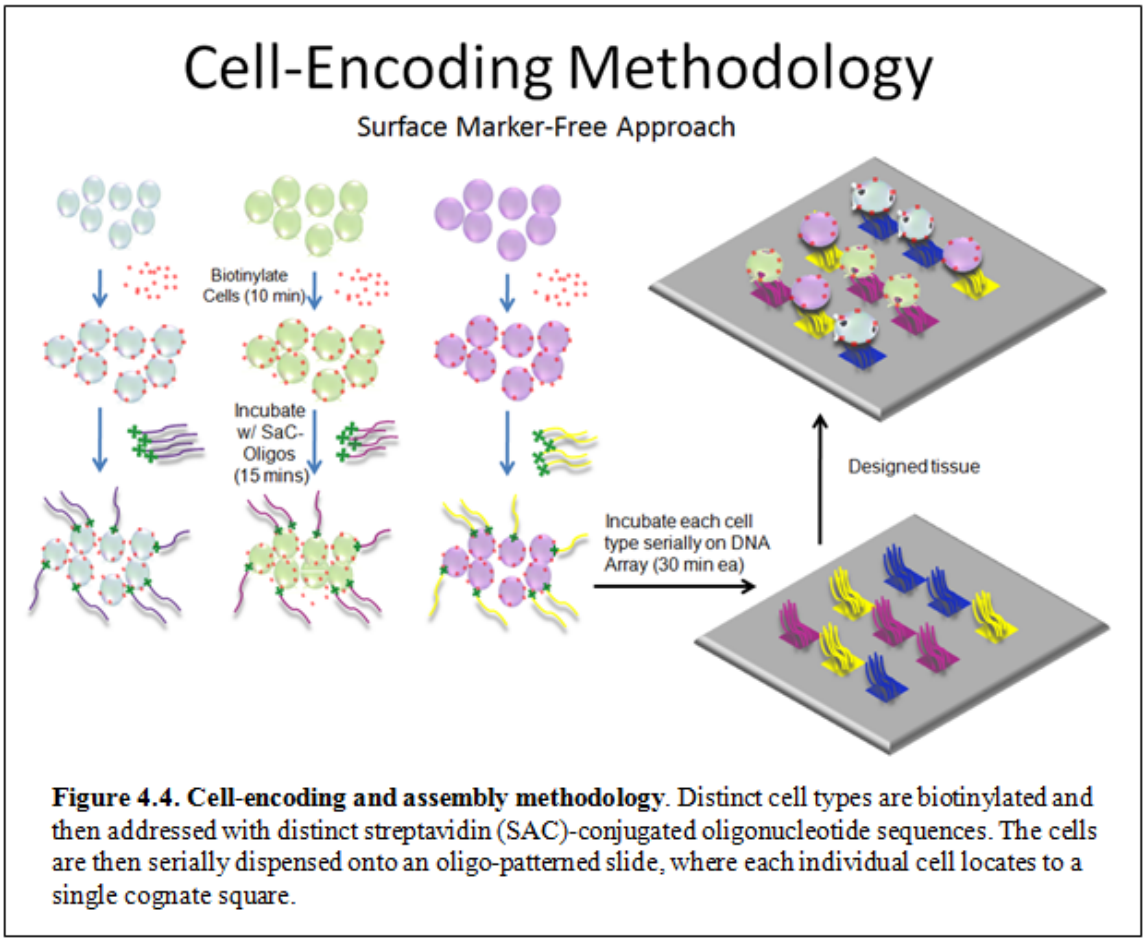

Figure 4.4. Cell-encoding and assembly methodology. Distinct cell types are biotinylated and then addressed with distinct streptavidin (SAC)-conjugated oligonucleotide sequences. The cells are then serially dispensed onto an oligo-patterned slide, where each individual cell locates to a single cognate square.

4.2.4 Patterning human central nervous system and mouse pancreatic islet tissue constructs

We first applied our patterning methodology toward creating a cell model of the human nervous system by co-assembling neurons and astrocytes into designed structures. The human CNS and neuronal systems in general are composed of neurons and glial cells interspersed in specific spatial organizations that are vital for the development of these systems[53]. Prior to integrating both cell types together, we first separately demonstrated the spatially selective capture of single astrocytes and single neurons. Primary human astrocytes were first encoded with **ii'** DNA and then incubated onto a 3 x 3 DNA microarray. The astrocytes localized only to the **ii** DNA squares, with ~27 % of squares covered by one astrocyte each). The fraction of squares covered by two astrocytes was larger (~40 %) because the astrocytes exhibited rapid division in culture, thus astrocytes that were dividing but hadn't completed mitosis could bind to a single spot (**Figure 4.5a**). Nonspecific binding of cells to non-cognate squares or to any other portions of the slide was not observed. In some cases, 3 to 4 astrocytes were found on particular **ii** DNA squares, which could be due to variability in the size of the astrocytes as well as the fact that astrocytes tend to cluster into small groups in culture. Astrocyte division was observed to continue on-chip even after the cells were patterned. In a separate experiment, primary human neurons were patterned onto the **iii** DNA spot of a 3 x 1 microarray (consisting only of oligo sequences **i**, **ii**, and **iii** as the capture sequences) to illustrate the extent of cell density (**Figure 4.5b**). A much higher percentage of the DNA squares (60 %) bound to only one cell relative to the astrocyte experiment since the neurons did not divide in culture. The cell-patterned slide was then incubated in media at 37 ^{o}C. When reassessed after 2 days, the neuronal processes were observed to be actively

growing, demonstrating that the neurons were still viable. Once the neurons were established, primary human astrocytes conjugated to **ii'** DNA were then incubated with the neuron-patterned slide and localized to their cognate squares. The final cell pattern consisted of multiple rows of primary human neurons and astrocytes spaced 30 µm apart, with each cell localized to a 10 µm x 10 µm DNA square (**Fig. 4.5c**). After incubation with astrocytes, it was clear based on cell morphology that the astrocytes were localized to the **ii** DNA squares, while the neurons remained on the **iii** DNA squares and did not move or get washed away from their initial designated locations.

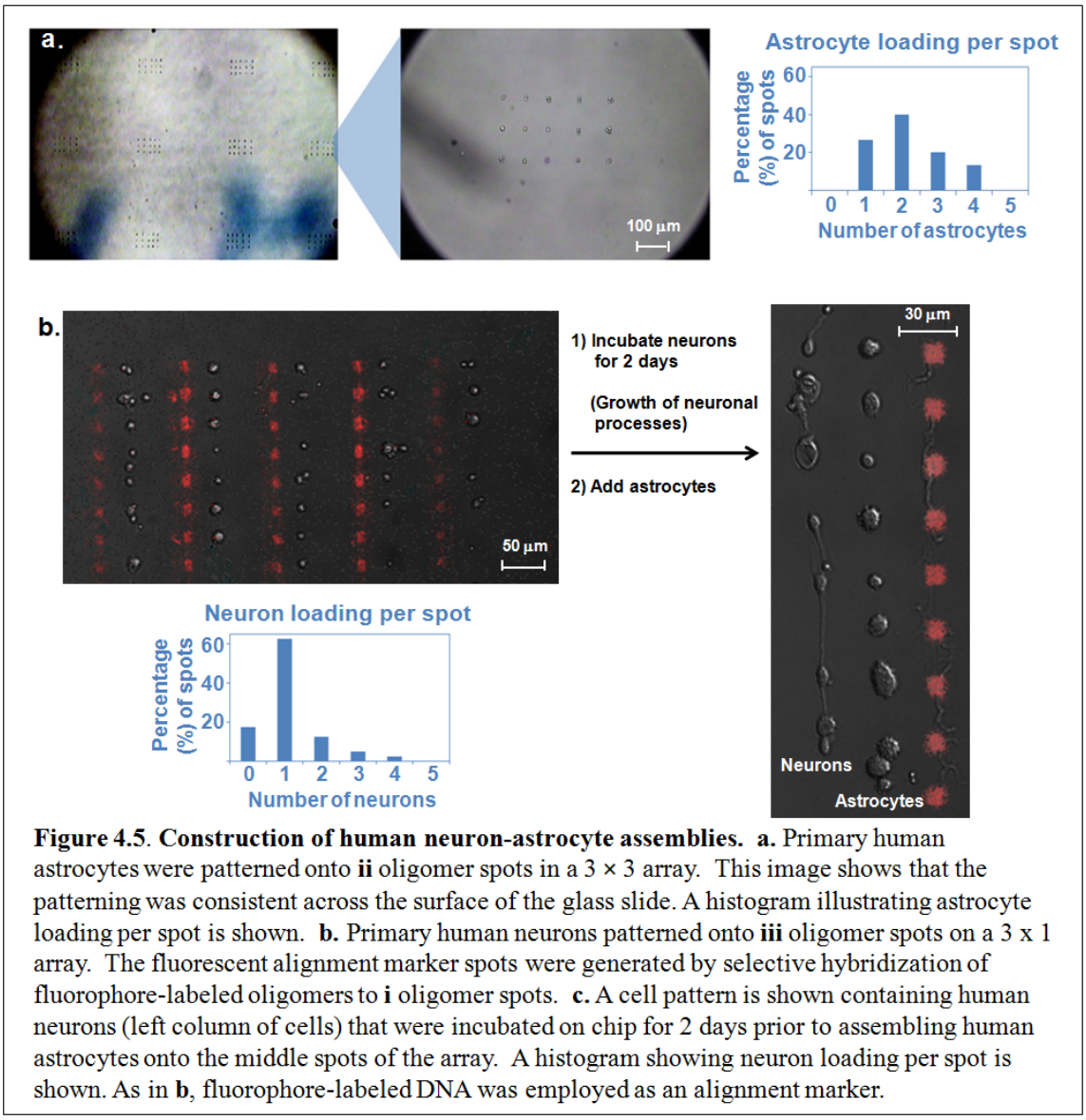

Figure 4.5. Construction of human neuron-astrocyte assemblies. **a.** Primary human astrocytes were patterned onto **ii** oligomer spots in a 3 × 3 array. This image shows that the patterning was consistent across the surface of the glass slide. A histogram illustrating astrocyte loading per spot is shown. **b.** Primary human neurons patterned onto **iii** oligomer spots on a 3 x 1 array. The fluorescent alignment marker spots were generated by selective hybridization of fluorophore-labeled oligomers to **i** oligomer spots. **c.** A cell pattern is shown containing human neurons (left column of cells) that were incubated on chip for 2 days prior to assembling human astrocytes onto the middle spots of the array. A histogram showing neuron loading per spot is shown. As in **b**, fluorophore-labeled DNA was employed as an alignment marker.

We also explored the construction of model pancreatic tissues. Some 340,000 people nationwide have diabetes mellitus type 1, which is characterized by loss of insulin production as a result of an autoimmune destruction of β cells within the pancreatic islets of Langerhans[54]. While pancreas transplants have proven to be effective in restoring normoglycemia in diabetic patients, this approach carries the risks attendant to major surgery and lifelong immunosuppression[55]. Allogeneic islet cell transplantation is a less invasive alternative, but typically is limited to patients with highly specific clinical

indications that are in addition to diabetes[55]. A promising alternative is to propagate and differentiate stem cells in culture into mature islet cells, thus yielding an unlimited number of transplantable cells[56]. However, all endocrine cell types in human islets, including the insulin-secreting β cells, the glucagon-secreting α cells, and the less abundant δ and PP cells, are arranged in apparently nonrandom architectures. We thus chose to explore our high resolution tissue engineering approach for mimicking the native islet microarchitectures.

In an effort to build a tissue that closely emulates the arrangement of cells in the human islets of Langerhans, we created an islet construct that included two mouse islet cell lines (α and β cells) patterned on the **iii** and **ii** DNA squares, respectively, of a 3 x 1 microarray with identical dimensions to that used for the neuron-astrocyte construct (**Figure 4.6**). As in the neuron-astrocyte cell patterning experiment, the α and β cells localized to their cognate DNA squares, typically averaging ~1 cell per square (~67 % of **iii** squares bound to only 1 α cell; ~87 % of **ii** squares bound to only 1 β cell). For every 100 correctly patterned cells, on average, only 1 cell bound nonspecifically, although there were examples of 2 or 3 cells patterning on a given spot (**Figure. 4.6a,b**).

We were able to designate a fraction of our arrays for conducting functional assays on the patterned cells. After the islet cells were patterned, **i'** DNA conjugated anti-insulin antibodies were incubated on the slide and allowed to hybridize to their cognate squares adjacent to the cells. The cells were incubated for 2 days to allow ample time for secreted insulin to bind to the anti-insulin antibody squares. The insulin assays were developed with biotinylated secondary antibodies followed by fluorophore-conjugated

streptavidin. The antibody squares fluoresced under confocal microscopy only when β cells were present (**Figure 4.6a-c**).

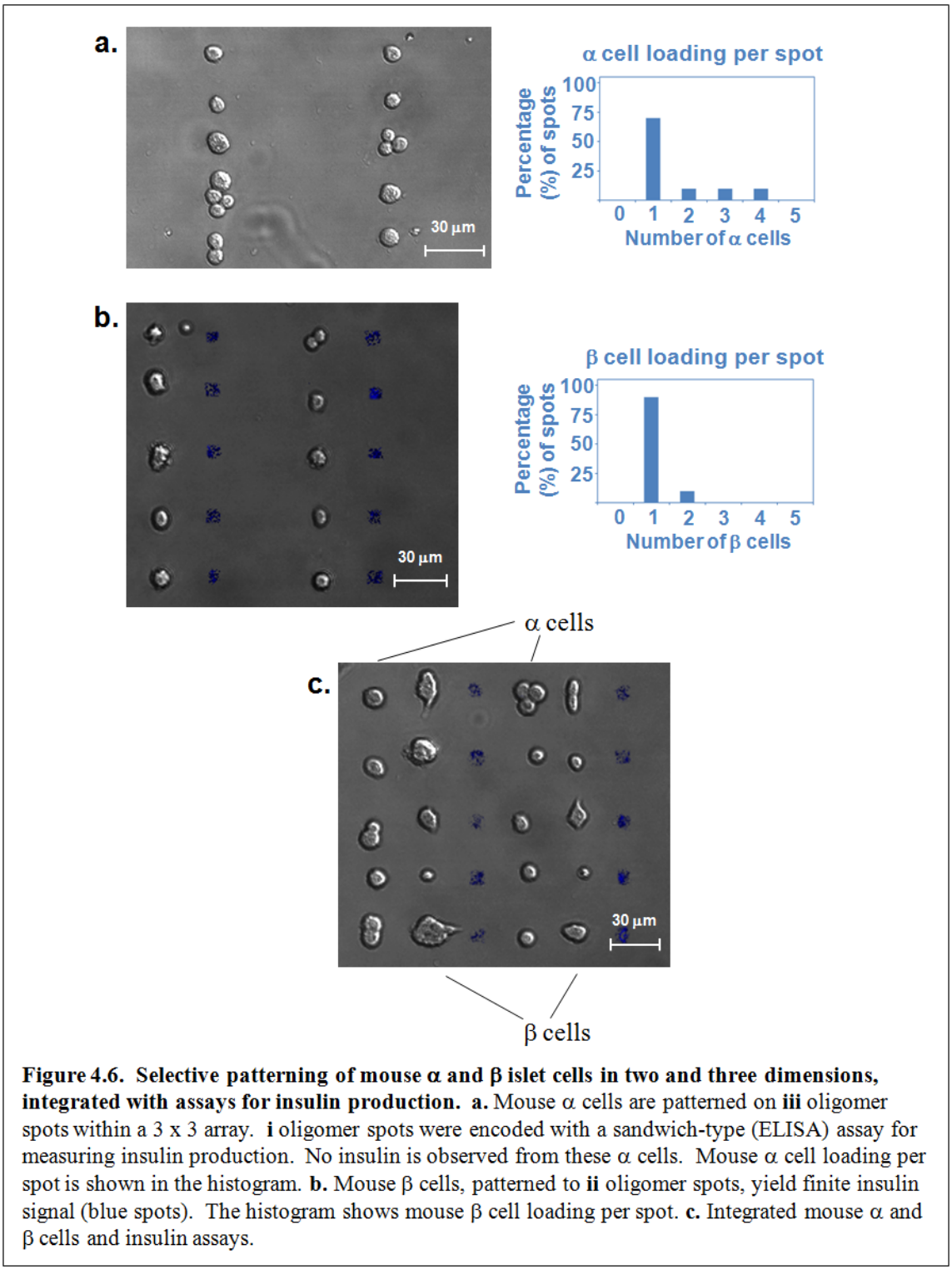

Figure 4.6. Selective patterning of mouse α and β islet cells in two and three dimensions, integrated with assays for insulin production. a. Mouse α cells are patterned on **iii** oligomer spots within a 3 x 3 array. **i** oligomer spots were encoded with a sandwich-type (ELISA) assay for measuring insulin production. No insulin is observed from these α cells. Mouse α cell loading per spot is shown in the histogram. **b.** Mouse β cells, patterned to **ii** oligomer spots, yield finite insulin signal (blue spots). The histogram shows mouse β cell loading per spot. **c.** Integrated mouse α and β cells and insulin assays.

Finally, we applied our platform to create islet tissue constructs in a 3-D configuration in order to more closely mimic native islet structures. Prior studies have shown that cell patterns can be encased in thin UV-curable polyethylene glycol (PEG) hydrogels and stacked to form 3-D tissue constructs.[8,57] In those studies, the cells are typically localized to the surface by nonchemical means such that cell-pattern transfer from the slide surface to the hydrogel layer is straightforward. In our case, the cells are chemically attached to the slide surface via DNA hybridization, and so it was not obvious that the cells could be readily transferred. However, we found that once the cell patterns were encased within a UV-cured PEG hydrogel, we were able to remove the cell-laden hydrogel layer from the glass surface without disturbing the cell pattern or damaging the cells. We aligned and stacked two such hydrogel layers to create a 3-D islet tissue construct (**Fig. 4.7**). This procedure could be repeated to build up multiple layers. Viability of the encased cells, as determined by calcein AM/ethidium homodimer (live/dead) staining, was confirmed after incubation in media at 37 ^{o}C for one week (**Fig. 4.7**). However, as in previous studies[8,57], cell division and mobility within the hydrogel matrix was not observed, likely due to the strong mechanical barrier provided by the rigid PEG membrane. The use of lower PEG concentrations or reduced UV light power would likely decrease this mechanical barrier, but at the expense of the rigidity needed to maintain the pattern integrity.

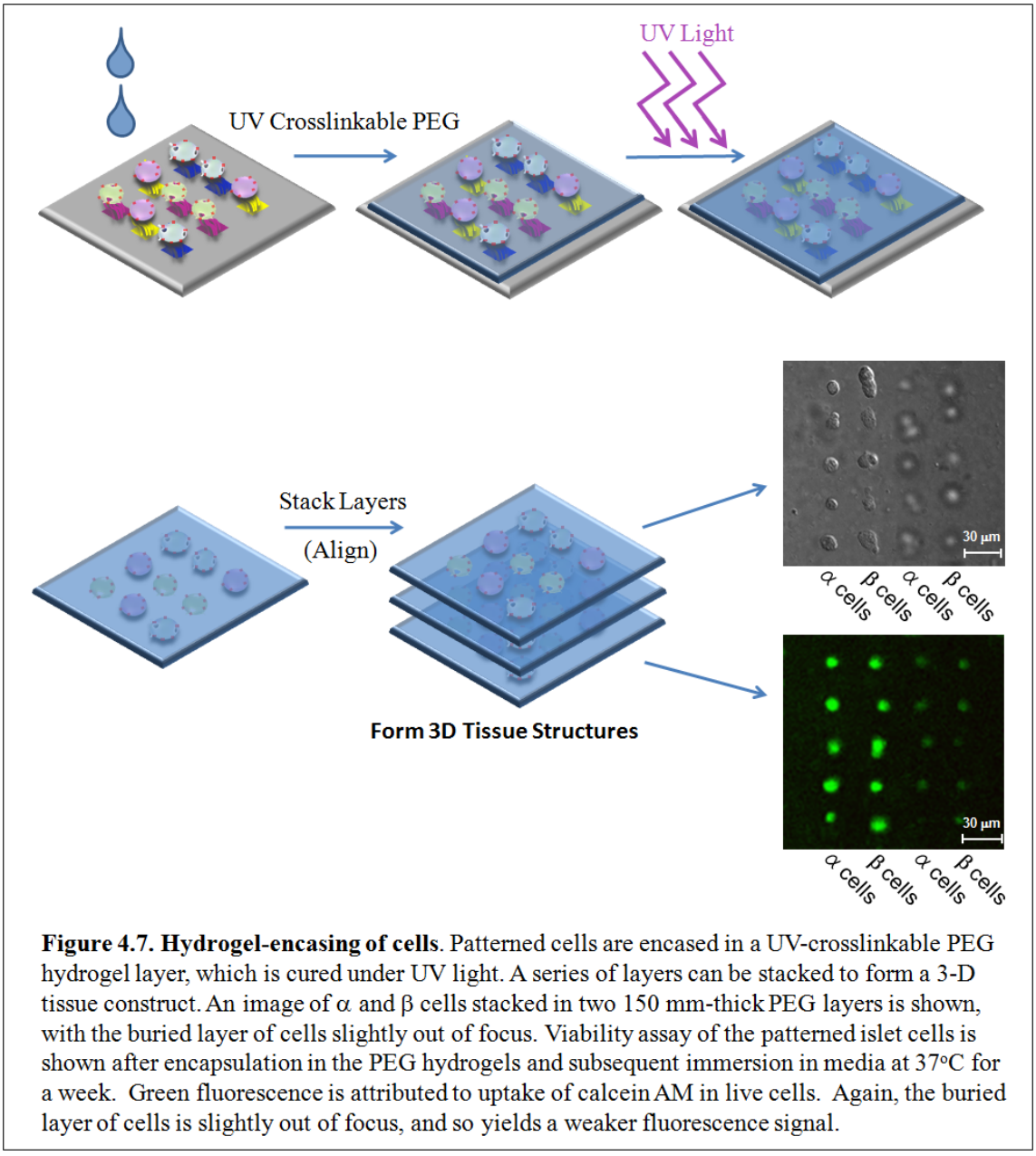

Figure 4.7. Hydrogel-encasing of cells. Patterned cells are encased in a UV-crosslinkable PEG hydrogel layer, which is cured under UV light. A series of layers can be stacked to form a 3-D tissue construct. An image of α and β cells stacked in two 150 mm-thick PEG layers is shown, with the buried layer of cells slightly out of focus. Viability assay of the patterned islet cells is shown after encapsulation in the PEG hydrogels and subsequent immersion in media at 37°C for a week. Green fluorescence is attributed to uptake of calcein AM in live cells. Again, the buried layer of cells is slightly out of focus, and so yields a weaker fluorescence signal.

The ability of our platform to act as an on-chip multiplexed ELISA technology could allow for a multitude of applications on densely patterned islet cells. For example, insulin levels could be compared to those of a series of control cultures containing equal amounts of the same 2 cell types in an unpatterned mixture of similar cell density: 1. in a culture dish (single layer of adherent cells); 2. in a single layer of cells encased in a

hydrogel; and 3. in a stacked 3-D structure. An identical set of control experiments could be carried out on *patterned* cells. Comparing insulin levels between experiments 1 and 2 would allow one to assess the effects on insulin-production of encasing islet cells in a hydrogel layer in both patterned and unpatterned scenarios. Comparing experiments 2 and 3 would allow one to determine the effect on insulin production of stacking multiple 2-D islet layers on top of each other (again in both patterned and unpatterned scenarios). Comparing patterned and unpatterned structures – be they un-encased, encased in a single hydrogel layer, or encased in a 3D hydrogel structure – would reveal whether maintaining the relative positions of the 2-cell types in 2-D and in 3-D has an effect on insulin production that differs from a structure containing a random mixture of the same cells.

A fourth experiment could compare insulin production by patterned 3-D structures comprised of aligned vs. unaligned cell layers. The cell-laden hydrogel layers could be aligned to each other using alignment markers (and a mask aligner), so that a given cell type always encounters the same neighboring cell in the layer above it (for example, a β cell in layer 2 is always above an α cell in layer 1). Such an experiment would show whether maintenance of a set cell configuration in all 3 axes of a 3-D islet tissue construct is functionally important (e.g. has an effect on insulin production) as compared with just 2 of the 3 axes.

A fifth experiment would compare insulin production by 3-D tissue constructs with that of islets isolated from a mouse. The mouse islets would be sectioned such that they contain the same number of cells as the engineered tissues. In all of the experiments just mentioned, glucagon functional assays could be performed for the other cell type (α cell) as well.

Furthermore, two-color fluorescence immunostaining for insulin and glucagon (α and β cells, respectively) could be performed on cut sections of the patterned single-layer and 3-D constructs on a routine basis. The intensity and distribution of immunostaining in these sections could provide additional functional information that ELISA could not. For example, on chip ELISA assays may not be sensitive enough to detect insulin production from a relatively small number of patterned cells. In addition, if insulin levels in the tissue media are low, it would be useful to know whether the problem is that: 1. the β cells are producing little or no insulin, or 2. the β cells are producing insulin but cannot secrete it. Both of these scenarios would be problematic in the context of a transplant, and would require further tinkering with the design parameters. Immunostaining would also show whether cells have migrated or otherwise deviated from their original configuration on the slide or in the hydrogel. These experiments could continue to be repeated for at least a month or for as long as the cells are viable.

4.3 Experimental Methods

4.3.1 Mold and device fabrication

Briefly, a 5-inch chrome mask drafted with the mold design (using AutoCAD software) and 4-inch silicon wafers were sent to a semiconductor processing foundry (Integrated Systems, Inc. ISSYS) for DRIE processing to create a silicon hard mold with 40 μm thick features. The design consisted of a series of twenty 10-μm wide serpentine channels (with 3 turns) spaced 30 μm apart. The hard mold was then placed in a chlorotrimethylsilane (TCMS) vapor chamber for 20 minutes. A PDMS mixture (10 parts

Sylgard 184 A:1 part Sylgard 184 B curing agent) was poured onto the mold in a petri dish, degassed for 1 hour in a vacuum dessicator, and then baked at 80 ^{o}C until the samples were softly cured (~20 min). The PDMS mold replica was then cut out of the bulk PDMS and through-holes were punched at the locations of the channel inlets and outlets. The microfluidic mold replica was then rinsed with IPA and DI water, airgun dried, and dust was removed with scotch tape. The device was then centered on a clean polylysine-coated glass slide and bonded by baking for 4 hours at 80 ^{o}C.

4.3.2 Validation of oligonucleotide set

The oligonucleotide sequences were chosen based on a pre-validated set of 12 orthogonal 40-mer oligos, each containing a unique 20-mer sequence followed by a 20-mer poly-A tail. These oligos had originally been screened for having very low calculated melting temperatures for hair-pin structures, self-hybridization, and cross-hybridization. Three of the sequences served as anchor sequences, with their complements serving as the “tail” portions of the bridging sequences. The other 9 sequences served as the “head” portions of the bridging sequences, with their complements serving as the conjugate strands for the cells. The 20-mer head and tail sequences were appended to each other via a 20-mer polyA sequence, creating a 60-bp bridging sequence. For the anchor oligonucleotides, a length of 80 base pairs (two identical 40-mer sequences (appended end-to-end) was found to be optimal in ensuring sufficient contact area with the polylysine surface to anchor the cells.

4.3.3 First flow-patterning step

1. 100 μM solutions of oligos **A**, **B**, and **C** ("anchor" sequences) were flowed into channels 1, 2, and 3 respectively. This was simultaneously repeated for each additional set of three channels. The solutions were flowed in at around 3 psi via external 23-gauge pin adapters connected to Tygon lines, which were hooked up to an external pressure source and pressure gauge. The solutions were flowed until 1 μL droplets formed at the outlets, indicating the channels were completely filled.
2. The device was then stored in a dessicator at room temperature for 2 days to allow for complete evaporation of water, leaving behind the DNA stripes on the substrate.
3. The PDMS was then peeled away and the patterned glass slide was baked at 80 ^{o}C for 2 – 4 hours to facilitate DNA bonding to the polylysine-coated slide.
4. In the meantime, a second PDMS mold replica was fabricated and rinsed thoroughly with IPA and DI H_2O, then airgun dried, and dust was again removed using scotch tape.
5. Once removed from the oven, the slide was allowed to cool to room temperature and rinsed briefly with DI H_2O to remove excess salts and unbound DNA, then dried with an airgun.
6. The second PDMS mold replica was then placed on the patterned slide oriented 90^{o}-clockwise with respect to the original position of the first PDMS mold replica in the first patterning step.
7. The device was then baked at 80 ^{o}C for 4 hours (for stronger bonding)

4.3.4 Second flow-patterning step

1. 3 % BSA/PBS blocking buffer was then flowed into all device channels for one hour at 3 psi.
2. For 3 x 3 Arrays: Solutions 1, 2, 3 (bridging sequences) were flowed into channels 1, 2, and 3, respectively, for one hour at 3 psi. This was simultaneously repeated for each additional set of three channels in the device. **Solution 1**: 50 µM each of oligo strands **A'-i**, **B'-ii**, **C'-iii**; **solution 2**: 50 µM each of oligo strands **A'-iv**, **B'-v**, and **C'-vi**; **solution 3**: 50 µM each of oligo strands **A'-vii**, **B'-viii**, and **C'-ix**.
3. For 3 x 1 Arrays: Solution 1 was flowed into multiple adjacent channels.
4. 3 % BSA/PBS buffer was then flowed into each channel for 1 hour to remove excess unbound DNA.
5. The PDMS was then peeled off, and the slide was incubated in a 3 % BSA/PBS bath (to block areas previously in contact with the PDMS), followed by rinsing with PBS, and airgun drying. (Rinsing with DI water was avoided at this step because it could dissociate the hybridized anchor and bridging strands).

4.3.5 DNA microarray validation

Once these DNAs were patterned into densely packed 3 x 3 grids or 3 x 1 grids, the patterned slide underwent a second cross-talk validation assay (now using just the 9 dye-conjugated complements **i'** through **ix'**) to ensure that no new crosstalk had been introduced by having two orthogonal sequences tethered into a single bridging sequence. This assay also served to assess whether there was leakage between microfluidic

patterning channels, which would manifest as smearing of the fluorescent signal between oligo squares in the grid.

4.3.6 Conjugating cells with DNA

1. Prior to conjugation, media was decanted from the cell culture dishes and the dishes were rinsed 3 times with 1x PBS.
2. Each dish was then incubated at room temperature for 10 minutes with 3 mL of a 40 μM solution of NHS-biotin in PBS (Solulink protocol).
3. The culture dishes were then rinsed 3 times with media to remove excess unreacted biotin.
4. 3 μL of 1 mg/mL SaC-oligo in 1 mL of 3 % BSA/PBS was added to each dish, followed by incubation at 37 ^{o}C for 5 minutes. The biotin-streptavidin binding reaction is complete in under 1 minute, but the reaction can proceed longer without causing harm to the cells. **iii'**-SaC was used to address α cells and neurons; **ii'**-SaC was used to address β cells and astrocytes.
5. The culture dishes were then rinsed again with 3 % BSA/PBS 3 times to remove excess unbound SaC-oligo.
6. 3 mL of warm (37 ^{o}C) trypsin was added to each culture dish and allowed to incubate for 3 minutes at 37 ^{o}C (to detach cells), followed by 5 mL trypsin-neutralizing solution and 5 mL of media.
7. Each cell suspension was then centrifuged at ~150 RCF for 5 min in a 15 mL falcon tube. The supernatant was aspirated, and oligo-conjugated cells were resuspended at a concentration of 10 million cells / mL in 2 μM EDTA in 3 % BSA/PBS.

4.3.7 Cell culture

All cell cultures were incubated in a 37 ^{o}C humidity-controlled incubator with 5 % CO_2/95 % air. Mouse cell-line derived pancreatic α cells (alpha TC1 clone 6, ATCC, Manassas, VA) were cultured in DMEM (Invitrogen Cat. No. 31600-034) containing: 10 % FBS (heat-inactivated), 15mM HEPES, 0.1 mM non-essential amino acids, 0.02 % BSA, 1.5 g/L sodium bicarbonate, 3.0 g/L glucose. Mouse cell-line derived pancreatic β cells (Beta-TC-6, ATCC) were cultured in 15 % FBS/DMEM. Experiments were conducted a week after plating. Human Primary Neurons (ScienCell Research Labs, Carlsbad, CA) were cultured in Neuronal Medium (ScienCell), and used for experiments 2 days after plating. Human Primary Astrocytes (ScienCell) were cultured and continued to divide in Astrocyte Medium (ScienCell) and were used 4 days after plating.

4.3.8 Cell patterning

Serial Processing:

1. Two distinct experiments were carried out, one with neurons and astrocytes and one with α cells and β cells
2. 200 µL of a single oligo-conjugated cell type (2 million cells total) was pipetted onto a pre-blocked ultra-dense oligo-patterned slide, followed by incubation at 37 ^{o}C for 30 min.
3. The cell-patterned slide was then swirled lightly in 3 % BSA/PBS to remove non-specifically bound cells.
4. This procedure was then repeated on the same slide (either immediately or within a couple days) using the second oligo-conjugated cell type.

5. A dye-conjugated DNA reference marker (50 nM **i'**-Cy3) was added prior to patterning of the cells to assess whether the cells were binding to the correct squares (relative to the reference marker).

4.3.9 Cell binding specificity

To assess whether oligo-conjugated cells bind only to their cognate DNA spots requires either that the morphologies of the patterned cell types be sufficiently distinct to be discernable under conventional light microscopy, or that each cell type be labeled with a distinct (fluorescent) marker. In this case, neurons and astrocytes could be clearly distinguished based on morphology. Likewise, α and β cells could be easily distinguished based on morphology. However, if fluorescent labeling were desired, it could be accomplished prior to the cell-patterning step by labeling the two cell types with distinct membrane-permeable dyes (e.g. Blue, Yellow, or Red Cell-Labeling Solutions from Molecular Probes: DiO, DiI, and DiD). Based on the cells' positions relative to the reference square (on examination under a fluorescent confocal microscope), one can straightforwardly determine whether each cell type has bound to the correct squares. Multiple array units can be examined to statistically analyze patterning reliability.

4.3.10 Hydrogel encapsulation of cells[8]

1. A 10 % solution of PEG-DA (MW 3400) in DMEM was filtered through a filter membrane with 0.2 μm pores.
2. Separately, 30 mg of 2,2-Dimethoxy-2-phenylacetophenone (DMPA) photoinitiator was dissolved in 100 μL N-vinylpyrrolidone.

3. 10 µL of DMPA solution was then added to 1 mL of PEG-DA solution and vortexed.
4. 150 µm-thick polished glass coverslips were then placed on the cell-patterned polylysine slide on either side of the cell-patterned area. A third coverslip was positioned such that it bridged the first two, creating a channel in which the cell-patterned glass substrate served as the floor, and the 3 coverslips served as the walls and ceiling.
5. The PEG pre-polymer solution was then pipetted into this channel and cured for 5 minutes under a UV lamp at 4 mW/cm^2 to form a thin (50 µm) hydrogel layer encasing the cells. The hydrogel layer was then peeled off keeping the cell pattern within intact.
6. By stacking multiple such layers on top of each other either with or without alignment, a three-dimensional tissue-like structure could be created.
7. The single-layer tissue or 3-D tissue construct was then placed in a culture dish with media.

4.3.11 Cell function assessment

Approximately 200 µL of a 5 µg/mL **i'**-anti-insulin Ab (R&D Systems, Minneapolis, MN) DNA-antibody conjugate in 15 % FBS/DMEM media solution was added to an islet cell patterned slide and allowed to hybridize to the squares of **i** DNA, followed by incubation at 37 ^oC for 2 days to allow insulin from nearby β cells to bind the conjugate. The slide was then gently rinsed three times with media followed by addition of a 200 µL solution of 2 µg/mL biotinylated insulin detection antibody (GeneTex, Irvine, CA) in media, which was allowed to incubate at 37 ^oC for 1 hour.

Again, the slide was gently rinsed three times with media, followed by a 1 hour incubation at 37 ^{o}C of a 200 µL solution of 5 µg/mL streptavidin-Cy5 conjugate (eBioscience, San Diego, CA) for fluorescence detection. A final triple rinse with media was performed.

4.4 Discussion

The proper functioning of tissues depends on the precise architectural arrangement of various cell types, facilitating the types of cell-cell interactions necessary for cell growth, differentiation, survival, migration, and regulation of tissue function. Consequently, it is believed that by mimicking the cellular and extracellular microarchitectural arrangements found in native tissues and organs, it will be possible to engineer substitutes that exhibit the same or very similar functions. The ability to arrange cells and cell types at single-cell resolution, as shown here, would enable new opportunities to more accurately mimic complex microarchitectures, like those seen in pancreatic islets, nervous tissue, and other organs.

It would be beneficial to see the islet cell construct function as well as native islet tissue. For one thing, human pancreatic islets consist predominantly of β (60 %) and α cells (30 %), with δ and PP cells constituting a small minority[23]. The construct shown here contains a distinct cell type on each of 2 squares in a repeating 3 x 1 array to demonstrate the multiplexing capability of the platform. As a result, both cell types are found in equal densities. This also means that, whereas native tissue consists predominantly of β cell / β cell, α cell / α cell, and α cell / β cell interactions, both cells types in the tissue constructed here could always interact with each other. Another

consequence of having equal numbers of each cell type is that the number of insulin-secreting β cells per unit volume of tissue is lower than in the native tissue, which could impact the level of insulin secretion. Further diminishing the cell density per unit volume is the thickness of the hydrogel layers. Each 150 μm-thick hydrogel layer contains just a single layer of cells. Since the cells are about 10 μm in diameter on average, the resulting gap between cell layers in the 3-D construct is about 140 μm. This also results in intercellular contacts being possible only in the x-y plane but not in the z-direction.

To address these issues, there are various ways in which islet structure can be more closely mimicked. Since cellular arrangement is hypothesized to affect cell viability and insulin production, future experiments could examine the effects of varying the pattern and distribution of the various cell types. These variations could include: 1. a checkerboard pattern of α and β cells (somewhat like the human or monkey islet), with or without interspersed δ and PP cells at regular intervals; or 2. an inner core of β cells surrounded by an outer mantle of α cells, and to a lesser extent δ and PP cells, as in the "core-mantle" model of the mouse islet[23]. The number of cells in the core and mantle can be tuned by adjusting the feature sizes, or by increasing the number of spots in each grid unit.

Furthermore, methods of narrowing the spacing between layers could be explored so as to allow for cell-cell contacts in all three axes. The hydrogel layer thickness is determined by the thickness of the coverslips used as the templates. Once 10 μm-thick coverslips are attainable, the hydrogel layer thickness will permit cell contacts in all 3 axes. In principle, an alternative would be to run a cell/PEG-prepolymer solution through a 10 μm-high microfluidic channel over the DNA patterned glass surface. Once the cells

bind to their cognate squares, the PEG matrix around them would be cured under UV. The PDMS would then be peeled off, leaving a 10 μm-thick cell-laden hydrogel stacking layer. In addition, since islets tend to assume a spherical glandular structure, the various layers could be cut into circular sections of varying radii which, when stacked, form hemispherical or spherical structures. Alternatively, a 3-D construct created from equal-sized stacks could, upon completion, be cut or punched to produce numerous tiny cylinders, spheres, or hemispheres of tissue.

Additional experiments could also explore modifying the extracellular environment and vascularizing the constructs to extend tissue longevity. Covalent attachment of extracellular matrix proteins (collagen, laminin, fibronectin) or peptides (RGD, IKVAV) to the hydrogel matrix would more closely mimic the extracellular environment of islet cells and prevent anoikis (apoptosis due to lack of cell-cell or cell-ECM interaction). To create much larger stacks of patterned hydrogel layers would require some mechanism of adequately perfusing the various layers since diffusion becomes limiting in hydrogel systems within a few tens of microns. This might be accomplished by lithographically imprinting capillary-like microchannels in each PEG hydrogel layer. Inlet and outlet holes could then be punched at either end of the 3-D construct, allowing perfusion of the imprinted capillary bed and its adjacent cells. Alternatively, a multitude of spherically-cut tissue sections could be packed into a rigid, hollow casing (like beads in a column) which can be perfused with media or blood. If hooked up to an arterial supply, the blood would permeate through the micron-sized spaces between the beads much as it would through capillary beds in real tissues.

4.5 Conclusion

In summary, we have patterned ultra-dense DNA microarrays for multiplexed single cell resolution cell patterning with applications in tissue engineering. We created two tissue constructs, one made up of two human central nervous system cell types (neurons and astrocytes) and one consisting of two mouse pancreatic islet cell types (α and β cells). Cell viability was confirmed in both constructs, and cell function was established in the islet cell construct through the detection of insulin secretion. In addition, islet cells were successfully transferred into PEG hydrogels and assembled into 3D tissue structures. These results imply that this cell patterning technology has the potential to be utilized for tissue engineered implants in individuals with compromised organ function.

4.6 Future Outlook

In addition to enabling the engineering of constructs that mimic more complex native microarchitectures, this platform could also offer the unique opportunity to create customizable tissues with novel microarchitectures. In particular, this platform could facilitate precise positioning and contact between cells that might not ordinarily be found together in native tissues. For example, neurons could be patterned alongside stomach cells that produce obestatin – an appetite-suppressant protein – creating a tissue that could one day facilitate voluntary nervous system control over appetite suppression for obese individuals. Clearly, ligand and receptor modifications would have to be genetically engineered to allow for communication between cell types that ordinarily do

not communicate. Also, the numbers and ratios of cell types in an engineered tissue could be adjusted to optimize that tissue's performance. For example, the relative positions and ratios of oligodendrocytes and neurons patterned in a customized nervous tissue transplant could be adjusted to enable improved myelination, synaptic connections, and neuronal functionality.

Given the multiplexing resolution that this technology enables, the door would be opened to a broad spectrum of other applications outside of tissue engineering. For instance, it would be possible to conduct cell-cell communication assays involving detection of cytokines or other secreted proteins from different types of single cells. To illustrate, a single glioblastoma (GBM) cancer cell and a single macrophage could be positioned at diagonal corners of a 3 x 3 array unit. The other 7 squares within the array could be occupied by a series of anti-cytokine and anti-growth factor antibodies. The cells could be given a specified amount of time (48 – 72 hours) to communicate in the presence of a stimulatory factor (like LPS), after which point labeled detection antibodies would be introduced and the intensities of each secreted cytokine measured. As a control, the same experiments could be conducted on each cell separately (equivalent of a highly multiplexed ELISPOT) to compare the relative contributions of each single cell secretion profile to the secretion of the dual-cell system. Because each of these 3 x 3 array units are repeated hundreds of times on a single slide, large sample sizes are afforded for statistical analysis.

This platform could also open up new opportunities in cell-based sensing, drug testing, and drug discovery, as assays could be performed on multiple tissue types on the same slide. For example, one could bond a PDMS stamp containing 10 separate channels

on top of the densely patterned DNA array. Different cell types and combinations could then be introduced into each microfluidic channel, where the conjugated cells would localize to their cognate squares, resulting in a different tissue type within each channel. Once cultured for a few days within the channels (under constant flow of media), a test drug could be introduced into each channel, and the outflow medium as well as the cells themselves could subsequently be analyzed. In this manner, drug effects could be straightforwardly tested on a number of different cells, cell combinations, or tissues simultaneously.

Finally, this patterning technology could be used for whole-genome or whole-proteome analyses on minute sample sizes for research purposes or for point-of-care diagnostics (**Figure 4.8**). Considering the small feature sizes possible (10 μm squares with 30 μm pitch), a set of 40,000 genes or proteins could be profiled within a microfluidic channel that is 500 μm wide and a few centimeters long. Twice that number could be profiled in a channel with twice the length or width. Moreover, by varying the number of assay channels, multiple low-volume samples could each be assayed for thousands of genes or proteins on a single chip.

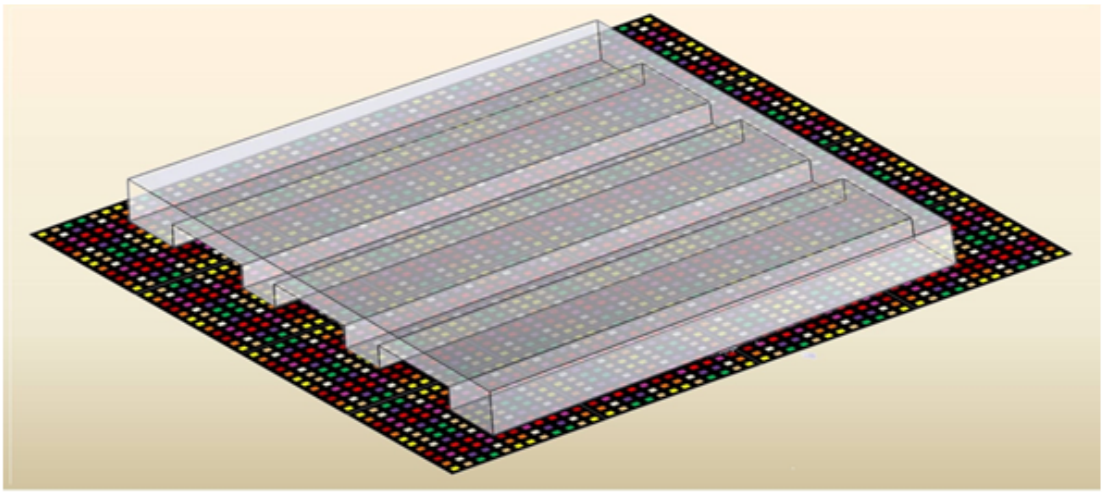

Figure 4.8. Scaled-up multiplexing. At the dimensions of the oligonucleotide squares (~10 μm resolution), hundreds or even thousands of distinct DNA strands could, in principle, be patterned within a single microfluidic channel, allowing for whole-genome and whole-proteome studies to be performed on extremely small (microliter) volumes within separate microfluidic channels.

4.7 References

1. Maemura, T.; Shin, M.; Sato, M.; Mochizuki, H.; Vacanti, J. A tissue-engineered stomach as a replacement of the native stomach. *Transplantation*, **2003**, 76, 61.

2. Grikscheit, T.; Ochoa, E.; Srinivasan, A.; Gaissert, H.; Vacanti, J. Tissue-engineered esophagus: experimental substitution by onlay patch or interposition. *J. Thorac. Cardiovasc. Surg.*, **2003**, 126, 537-544.

3. Vacanti, M. P.; et al. Tissue-engineered spinal cord. *Transplant Proc.*, **2001**, 33, 592-598.

4. Vacanti, J. P. Tissue and organ engineering: Can we build intestine and vital organs? *J. Gastrointest. Surg.*, **2003**, 7, 831-835.

5. Langer, R.; Vacanti, J. Tissue engineering. *Science*, **1993**, 920-926.

6. Boland, T.; Mironov, V.; Gutowska, A.; Roth, E.; Markwald, R. Cell and organ printing 2: fusion of cell aggregates in three-dimensional gels. *Anat. Rec. A Discov. Mol. Cell. Evol. Biol.*, **2003**, 272, 497-502.

7. Stegemann, J.; Kaszuba, S.; Rowe, S. Review: advances in vascular tissue engineering using protein-based biomaterials. *Tissue Eng.*, **2007**, 13, 2601-2613.

8. Albrecht, D.; Underhill, G.; Wassermann, T.; Sah, R.; Bhatia, S. Probing the role of multicellular organization in three-dimensional microenvironments. *Nat. Methods*, **2006**, 3, 369-375.

9. Tibbitt, M.; Anseth, K. Hydrogels as extracellular matrix mimics for 3D cell culture. *Biotechnol. Bioeng.*, **2009**, 103, 655-663.

10. Beck, J.; et al. Islet encapsulation: strategies to enhance islet cell functions. *Tissue Eng.*, **2007**, 13, 589-599.

11. Weber, L.; Hayda, K.; Anseth, K. Cell-matrix interactions improve β-cell survival and insulin secretion in three-dimensional culture. *Tissue Eng. A*, **2003**, 14, 1959-1968.

12. Ling, Y.; et al. A cell-laden microfluidic hydrogel. *Lab Chip*, **2007**, 7, 756-762.

13. Orive, G.; et al. Cell encapsulation: promise and progress. *Nat. Med.*, **2003**, 9, 104-107.

14. de Vos, P.; Marchetti, P. Encapsulation of pancreatic islets for transplantation in diabetes: the untouchable islets. *Trends Mol. Med.*, **2002**, 8, 363-366.

15. Weber, L.,; He, J.; Bradley, B.; Haskins, K.; Anseth, K. PEG-based hydrogels as an in vitro encapsulation platform for testing controlled [beta]-cell microenvironments. *Acta Biomater.*, **2006**, 2, 1-8.

16. Robitaille, R.; et al. Studies on small (< 350 μm) alginate-poly-L-lysine microcapsules. V. Determination of carbohydrate and protein permeation through microcapsules by reverse-size exclusion chromatography. *J. Biomed. Mater. Res. A*, **2000**, 50, 420-427.

17. Koh, W.; Revzin, A.; Pishko, M. Poly (ethylene glycol) hydrogel microstructures encapsulating living cells. *Langmuir*, **2002**, 18, 2459-2462.

18. Koizumi, S.; Fujishita, K.; Inoue, K. Regulation of cell-cell communication mediated by astrocytic ATP in the CNS. *Purinergic Signal*., **2005**, 1, 211-217.

19. Haydon, P. G. Glia: listening and talking to the synapse. *Nature Rev. Neurosci.*, **2001**, 2, 185-193.

20. Ransom, B.; Behar, T.; Nedergaard, M. New roles for astrocytes (stars at last). *Trends Neurosci.*, **2003**, 26, 520-522.

21. Jain, R.; Lammert, E. Cell–cell interactions in the endocrine pancreas. *Diabetes Obes. Metab.*, **2009**, 11, 159-167.

22. Le Marchand, S.; Piston, D. Glucose suppression of glucagon secretion. *J. Biol. Chem.*, **2010**, 285, 14389.

23. Cabrera, O.; et al. The unique cytoarchitecture of human pancreatic islets has implications for islet cell function. *P. Natl. Acad. Sci. USA*, **2006**, 103, 2334.

24. Shear, J.; et al. Single cells as biosensors for chemical separations. *Science*, **1995**, 267, 74.

25. Rider, T.; et al. AB cell-based sensor for rapid identification of pathogens. *Science*, **2003**, 301, 213.

26. Ziauddin, J.; Sabatini, D. Microarrays of cells expressing defined cDNAs. *Nature*, **2001**, 411, 107-110.

27. Beske, O.; Goldbard, S. High-throughput cell analysis using multiplexed array technologies. *Drug Discov. Today*, **2002**, 7, S131-S135.

28. Kleinfeld, D.; Kahler, K.; Hockberger, P. Controlled outgrowth of dissociated neurons on patterned substrates. *J. Neurosci.*, **1988**, 8, 4098.

29. Revzin, A.; Tompkins, R.; Toner, M. Surface engineering with poly (ethylene glycol) photolithography to create high-density cell arrays on glass. *Langmuir*, **2003**, 19, 9855-9862.

30. Cukierman, E.; Pankov, R.; Stevens, D.; Yamada, K. Taking cell-matrix adhesions to the third dimension. *Science's STKE*, **2001**, 294, 1708.

31. Singhvi, R.; et al. Engineering cell shape and function. *Science*, **1994**, 264, 696.

32. Chen, C.; Mrksich, M.; Huang, S.; Whitesides, G.; Ingber, D. Geometric control of cell life and death. *Science*, **1997**, 276, 1425.

33. Wilson Jr, W. & Boland, T. Cell and organ printing 1: protein and cell printers. *Anat. Rec. A Discov. Mol. Cell. Evol. Biol.*, **2003**, 272, 491-496.

34. Xu, T.; Jin, J.; Gregory, C.; Hickman, J.; Boland, T. Inkjet printing of viable mammalian cells. *Biomaterials*, **2005**, 26, 93-99.

35. Jiang, X.; Ferrigno, R.; Mrksich, M.; Whitesides, G. Electrochemical desorption of self-assembled monolayers noninvasively releases patterned cells from geometrical confinements. *J. Am. Chem. Soc.*, **2003**, 125, 2366-2367.

36. Lahann, J.; et al. A reversibly switching surface. *Science*, **2003**, 299, 371.

37. Ostuni, E.; Kane, R.; Chen, C.; Ingber, D.; Whitesides, G. Patterning mammalian cells using elastomeric membranes. *Langmuir*, **2000**, 16, 7811-7819.

38. Folch, A.; Jo, B.; Hurtado, O.; Beebe, D.; Toner, M. Microfabricated elastomeric stencils for micropatterning cell cultures. *J. Biomed. Mater. Res. A*, **2000**, 52, 346-353.

39. Rettig, J.; Folch, A. Large-scale single-cell trapping and imaging using microwell arrays. *Anal. Chem.*, **2005**, 77, 5628-5634.

40. Birkbeck, A.; et al. VCSEL arrays as micromanipulators in chip-based biosystems. *Biomed. Microdevices*, **2003**, 5, 47-54.

41. Dufresne, E.; Grier, D. Optical tweezer arrays and optical substrates created with diffractive optics. *Rev. Sci. Instrum.*, **1998**, 69, 1974.

42. Ozkan, M.; et al. Electro-optical platform for the manipulation of live cells. *Langmuir*, **2003**, 19, 1532-1538.

43. Rosenthal, A.; Voldman, J. Dielectrophoretic traps for single-particle patterning. *Biophys. J.*, **2005**, 88, 2193-2205.

44. Fan, R.; et al. Integrated barcode chips for rapid, multiplexed analysis of proteins in microliter quantities of blood. *Nat. Biotechnol.*, **2008**, 26, 1373-1378.

45. Erickson, D.; Li, D. Integrated microfluidic devices. *Anal. Chim. Acta*, **2004**, 507, 11-26.

46. Jo, B.; Van Lerberghe, L.; Motsegood, K.; Beebe, D. Three-dimensional micro-channel fabrication in polydimethylsiloxane (PDMS) elastomer. *J. Microelectromech S.*, **2000**, 9, 76-81.

47. Chandra, R.; Douglas, E.; Mathies, R.; Bertozzi, C.; Francis, M. Programmable cell adhesion encoded by DNA hybridization. *Angew. Chem. Int. Edit.*, **2006**, 45, 896-901.

48. Hsiao, S.; et al. Direct cell surface modification with DNA for the capture of primary cells and the investigation of myotube formation on defined patterns. *Langmuir*, **2009**, 25, 6985-6991.

49. Kwong, G.; et al. Modular nucleic acid assembled p/MHC microarrays for multiplexed sorting of antigen-specific T cells. *J. Am. Chem. Soc.*, **2009**, 131, 9695-9703.

50. Gard, A. L.; Pfeiffer, S. E.; Williams, I. Immunopanning and developmental stage-specific primary culture of oligodendrocyte progenitors (O4+ GalC) directly from postnatal rodent cerebrum. *Neuroprotocols*, **1993**, 2, 209-218.

51. Yang, P.; Hernandez, M. Purification of astrocytes from adult human optic nerve heads by immunopanning. *Brain Res. Protoc.*, **2003**, 12, 67-76.

52. Ingraham, C.; Rising, L.; Morihisa, J. Development of O4+/O1-immunopanned pro-oligodendroglia in vitro. *Dev. Brain Res.*, **1999**, 112, 79-87.

53. Yang, I. H.; Co, C.C.; Ho, C.-C. Spatially controlled co-culture of neurons and glial cells. *J. Biomed. Mater. Res.*, **2005**, 75, 976-984.

54. Fauci, A. *Harrison's Principles of Internal Medicine*. McGraw-Hill: New York, 2005.

55. Jones, P.; Courtney, M.; Burns, C.; Persaud, S. Cell-based treatments for diabetes. *Drug Discov. Today*, **2008**, 13, 888-893.

56. Burt, R. K.; Oyama, Y.; Traynor, A.; Kenyon, N. S. Hematopoietic stem cell therapy for type 1 diabetes: induction of tolerance and islet cell neogenesis. *Autoimmun. Rev.*, **2002**, 1, 133-138.

57. Liu, V. A.; Bhatia, S. N. Three-dimensional photopatterning of hydrogels containing living cells. *Biomed. Microdevices,* **2002**, 4, 257-266.

4.8 Appendix

To validate that the designed oligo set was truly orthogonal, cross-talk assays were performed on the twelve oligos. First, the twelve primary strands were array-spotted on a polylysine-coated glass slide, baked at 80 ^{o}C for 2 – 4 hours, rinsed briefly with DI water, and airgun dried. A thin slab of PDMS with 12 pre-cut square holes was then bonded to the spotted glass slide, forming 12 assay wells. The wells were then blocked with 3 % BSA/PBS for an hour. Twelve solutions, each containing 50 nM of a distinct dye-conjugated complementary strand in 3 % BSA/PBS, were prepared and pipetted into the wells, such that each well was incubated with a different complementary strand for an hour. An additional complementary oligo (also at 50 nM) with a distinct dye color was added at this step as a reference marker. The same reference marker was used in all twelve wells. The wells were then rinsed with 3 % BSA/PBS, the PDMS was peeled off, and the slide was rinsed with 1x PBS followed by DI water, then airgun dried. The slide was then scanned using a fluorescent microarray scanner to determine if more than one of the twelve spots fluoresced, suggesting cross-talk. If this occurred, the sequence assayed would be considered insufficiently orthogonal to the rest of the panel and would be replaced by a different sequence.

Our lab has previously validated a set of 12 orthogonal oligos, whose sequences (not including the 20-mer polyA tail) are shown below:

A	ATCCTGGAGCTAAGTCCGTA	A'	TACGGACTTAGCTCCAGGAT
B	GCCTCATTGAATCATGCCTA	B'	TAGGCATGATTCAATGAGGC
C	GCACTCGTCTACTATCGCTA	C'	TAGCGATAGTAGACGAGTGC
i	ATGGTCGAGATGTCAGAGTA	i'	TACTCTGACATCTCGACCAT
ii	ATGTGAAGTGGCAGTATCTA	ii'	TAGATACTGCCACTTCACAT
iii	ATCAGGTAAGGTTCACGGTA	iii'	TACCGTGAACCTTACCTGAT
iv	GAGTAGCCTTCCCGAGCATT	iv'	AATGCTCGGGAAGGCTACTC
v	ATTGACCAAACTGCGGTGCG	v'	CGCACCGCAGTTTGGTCAAT
vi	TGCCCTATTGTTGCGTCGGA	vi'	TCCGACGCAACAATAGGGCA
vii	TCTTCTAGTTGTCGAGCAGG	vii'	CCTGCTCGACAACTAGAAGA
viii	TAATCTAATTCTGGTCGCGG	viii'	CCGCGACCAGAATTAGATTA
ix	GTGATTAAGTCTGCTTCGGC	ix'	GCCGAAGCAGACTTAATCAC

The first 3 sequences (A, B, C) can serve as the anchor sequences, as follows:

2X A-3'-polyA

ATCCTGGAGCTAAGTCCGTAAAAAAAAAAAAAAAAAAAAATCCTGGAGCTAAGTCCGTAAAAAAAAAAAAAAAAAAAA

2X B-3'-polyA

GCCTCATTGAATCATGCCTAAAAAAAAAAAAAAAAAAAAGCCTCATTGAATCATGCCTAAAAAAAAAAAAAAAAAAAA

2X C-3'-polyA

GCACTCGTCTACTATCGCTAAAAAAAAAAAAAAAAAAAAGCACTCGTCTACTATCGCTAAAAAAAAAAAAAAAAAAAA

The complements to the anchors and the 9 remaining sequences can then be coupled together as follows:

A'-i TACGGACTTAGCTCCAGGATAAAAAAAAAAAAAAAAAAAAATGGTCGAGATGTCAGAGTA
B'-ii TAGGCATGATTCAATGAGGCAAAAAAAAAAAAAAAAAAAAATGTGAAGTGGCAGTATCTA
C'-iii TAGCGATAGTAGACGAGTGCAAAAAAAAAAAAAAAAAAAAATCAGGTAAGGTTCACGGTA
A'-iv TACGGACTTAGCTCCAGGATAAAAAAAAAAAAAAAAAAAAGAGTAGCCTTCCCGAGCATT
B'-v TAGGCATGATTCAATGAGGCAAAAAAAAAAAAAAAAAAAAATTGACCAAACTGCGGTGCG
C'-vi TAGCGATAGTAGACGAGTGCAAAAAAAAAAAAAAAAAAAAATGCCCTATTGTTGCGTCGGA
A'-vii TACGGACTTAGCTCCAGGATAAAAAAAAAAAAAAAAAAAAATCTTCTAGTTGTCGAGCAGG
B'-viii TAGGCATGATTCAATGAGGCAAAAAAAAAAAAAAAAAAAAATAATCTAATTCTGGTCGCGG
C'-ix TAGCGATAGTAGACGAGTGCAAAAAAAAAAAAAAAAAAAAGTGATTAAGTCTGCTTCGGC